

Structural and electronic properties of fluorinated double-walled boron nitride nanotubes: Effect of interwall interaction

Haitao Liu, Gang Zhou, Qimin Yan, Jian Wu, Bing-Lin Gu, and Wenhui Duan*
Department of Physics, Tsinghua University, Beijing 100084, People's Republic of China

Dong-Liang Zhao

Central Iron and Steel Research Institute, Beijing 100081, People's Republic of China

(Received 19 September 2006; revised manuscript received 16 January 2007; published 9 March 2007)

The mechanism of fluorine-functionalized multiwalled boron nitride nanotubes (MWBNNs) is studied through *ab initio* calculations for the structural and electronic properties of (8,0)–(16,0) double-walled structures. It is shown that the F atoms could be exothermically doped into the interstitial region between two adjacent tubes or adsorbed on the exterior surface of the outmost tube. Interstitial F doping can significantly change the interwall interaction and can lead to evident changes in structural and electronic properties of such doped system. As a result, both tube walls turn into effective conducting channels, which makes a significant contribution to the enhancement of electrical conductivity of fluorine-functionalized MWBNNs. In contrast, the F adsorption on the exterior surface of the outmost tube hardly alters the interwall interaction and only affects the structural and electronic properties of the outer tube wall. Our work indicates that the electronic properties of MWBNNs could be significantly modulated by adjusting the interwall interaction.

DOI: [10.1103/PhysRevB.75.125410](https://doi.org/10.1103/PhysRevB.75.125410)

PACS number(s): 73.22.-f, 73.20.Hb, 61.46.Fg, 68.43.Fg

I. INTRODUCTION

As one of the isoelectronic structures for carbon nanotubes (CNTs), boron nitride nanotubes^{1,2} (BNNTs) possess similar geometry and mechanical properties to CNTs due to identical σ bonds (sp^2 hybridization), but have different electronic properties and chemical activities from CNTs, resulting from different spatial distributions of π states in these two tubular structures. Especially, stable semiconducting behavior^{1,3} and outstanding chemical inertness⁴ of BNNTs make them suitable for nanoscale devices in harsh environments. On the other hand, BNNTs have a large optical gap of 5.8 ± 0.2 eV,³ which is strongly dominated by excitonic effects (electron-hole interaction),⁵ and their electronic band gap should be even considerably larger. This will hinder further electronic applications of BNNTs. Therefore, modifying electronic structures of BNNTs is crucial for transforming potentiality into actuality, and the associated scientific and technological innovations have attracted more and more interests. In comparison with nonchemical methods such as using the external force⁶ or electric field,⁷ doping with certain elements is one of the most promising ways for modification of electronic properties of BNNTs.⁸ Recently, Tang *et al.* succeeded in preparation of stable fluorinated BNNTs (F-BNNTs) and observed a great enhancement of electric conductance by a four-probe I - V measurement.⁹ From first-principles calculations of single-walled BNNTs (SWBNNTs), Xiang *et al.* suggested that such an enhancement could be induced by the adsorption of F atoms.¹⁰

In practice, BNNTs mostly have multiwalled structures.¹¹ Especially, the total amount of BNNTs with even number of shells was found to markedly prevail over that with odd number of shells.¹² It is noted that multiwalled nanotubes (MWNTs) exhibit different structural characteristics (especially the existence of the interstitial region between neighboring tubes) from single-walled nanotubes (SWNTs), in es-

sence, and the inherent interwall interaction could play an important role in the structural, electronic, and optical properties of MWNTs, even in their potential applications.^{13–15} Okada *et al.* theoretically demonstrated that the electronic structures of double-walled BNNTs (DWBNNs) are more complex than those of single-walled BNNTs (SWBNNTs).¹³ Typically, the resulting band structures are related to the tube radii as well as the rehybridizations between σ and π states. Jhi *et al.* found that the interwall stacking should play a significant role in the interwall interaction and in the formation of DWBNNs [or multiwalled BNNTs (MWBNNs)], and the fundamental energy gap of DWBNNs is smaller than that of SWBNNTs, mostly owing to band shift.¹⁴ Moreover, the second-order nonlinear optical coefficients of DWBNNs are significantly reduced by the interwall interaction, in comparison with SWBNNTs.¹⁵ Thus, it is very important to take into account the multiwalled structures for revealing the underlying physical phenomena,^{16,17} even though the interwall interaction might be weak. Also, it is expected that the transport behavior and mechanism of doped MWNTs are more complicated and could be different from those of doped SWNTs. Some fundamental questions will be raised naturally: How does extrinsic doping affect the interwall interaction? Is the structure or morphology of the doped MWNT only a simple combination of individual doped and pristine SWNTs? Are the electronic structures of different shells in MWNTs affected by dopants individually, or as a whole? However, previous theoretical studies of doping effect (such as F atoms) on electronic properties of BNNTs only focused on the single-walled structure,¹⁰ instead of the real physical circumstances of multiwalled structures.⁹

To address these fundamental issues, in this paper, we comprehensively study the modification mechanism of electronic structures of F-BNNTs by *ab initio* calculations on multiwalled structures (the DWBNN should be a good model, with an appropriate balance between computational

accuracy and effort). We especially focus on the structural and electronic properties of DWBNNT with interstitial F doping and demonstrate that there exists a quite different scheme of interwall interaction, as compared with the pristine DWBNNT. Moreover, as a comparative study, the F adsorption on the exterior surface of the outmost tube in DWBNNT is also investigated.

II. COMPUTATIONAL METHODS AND DETAILS

Our calculations are performed using the density-functional theory in the generalized gradient approximation, with the Perdew-Burke-Ernzerhof functional¹⁸ for the exchange and correlation effects of the electrons, as implemented in the Vienna *ab initio* simulation package.¹⁹ The electron-ion interaction is described by the projector-augmented wave method,²⁰ and the cutoff energy for the plane-wave basis set is 550 eV. In light of the previous experiment²¹ and theoretical study,¹³ we adopt the model of a zigzag (8,0)–(16,0) DWBNNT placed in a hexagonal supercell with lattice parameters of 25 Å in the x - y plane (note that the interaction between adjacent DWBNNTs could be negligible), and the length of unit cell along the tube axis is 4.34 Å. The $1 \times 1 \times 15$ Monkhorst-Pack \mathbf{k} -point mesh²² is used to sample the Brillouin zone. The residual minimization method with direct inversion of iterative subspace minimization scheme is utilized for electronic structure calculations. Structural optimizations are deemed sufficiently converged when the forces on all ions are less than 0.02 eV/Å, in virtue of the quasi-Newton algorithm.

III. RESULTS AND DISCUSSION

In order to reveal the underlying mechanism of fluorination-induced conductivity enhancement observed experimentally, two facts should be considered: (i) the experiment of Tang *et al.*⁹ for F-functionalized BNNTs was implemented in the synthesis process of MWBNNTs and (ii) the total surface area of interstitial regions of MWBNNTs (it should roughly linearly increase with the number of tube walls) is far larger than that of the exterior (interior) surface of the outmost (innermost) tube. It is believed that the interstitial region between neighboring tubes should be important for the actual doping. The DWBNNT [shown in Fig. 1(a)], the simplest multiwalled structure of BNNTs, is studied to understand the nature of MWBNNTs because the essential feature of interwall interaction in them is retained.²³ Then the F atoms are placed in the interstitial region or on the exterior surface of tubes for exploring the doping mechanism of F-BNNTs.²⁴ In one supercell, four F atoms are placed symmetrically (corresponding to a F-doping concentration of 4 at. %), either in the interstitial region [i.e., on the exterior surface of the (8,0) tube or on the interior surface of the (16,0) tube, denoted as the EXO-8 and INT-16 configurations, respectively] or on the exterior surface (denoted as the EXO-16 configuration) of the DWBNNT, as shown in Figs. 1(b)–1(d). The calculated binding energies²⁵ of the EXO-16, EXO-8, and INT-16 configurations are, respectively, -2.17 , -1.33 , and -0.47 eV/F atom (note that the negative binding

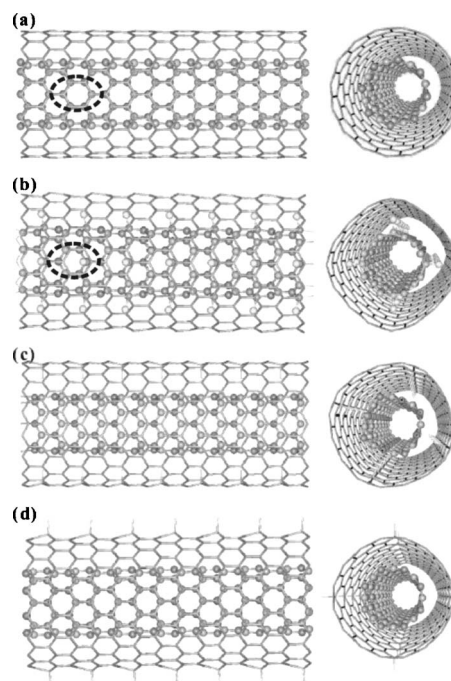


FIG. 1. (a) Schematic diagram of the pristine (8,0)–(16,0) DWBNNT. Three configurations of F-doped (8,0)–(16,0) DWBNNTs are shown: (b) four F atoms are adsorbed on the exterior surface of the inner (8,0) tube (“EXO-8”), (c) four F atoms are adsorbed on the interior surface of the outer (16,0) tube (“INT-16”), and (d) four F atoms are adsorbed on the exterior surface of the outer (16,0) tube (“EXO-16”). In each panel, the side and perspective views are shown in the left and right, respectively. Note that the outer and inner walls are represented with stick-only and ball-and-stick models, and the B, N, and F atoms are represented with the pink (dark gray), blue (black), and cyan (light gray) balls and sticks. The enlarged schematic diagrams of the elliptical domains in (a) and (b) will be shown in Figs. 2(e) and 2(f), respectively.

energy corresponds to the exothermic reaction, and these values imply that all these F-doping configurations are energetically favorable). Evidently, in the case of interstitial doping, the F atoms prefer to adsorb on the exterior surface of the (8,0) tube (i.e., the EXO-8 configuration), rather than on the interior surface of the (16,0) tube (i.e., the INT-16 configuration). This should be related to the different σ - π hybridization extent of these tube walls determined by their curvatures.¹³ In addition, it can be expected that the energy difference between the two configurations of interstitial doping decreases with increasing tube diameters. On the other hand, the interstitial F doping will induce a more significant structural deformation than the F adsorption on the exterior surface of the outmost tube in DWBNNT, and the energy difference induced by the curvature effect is much smaller than the strain energy induced by interstitial F doping. Therefore, the EXO-16 configuration (with F adsorption on the exterior surface of DWBNNT) is energetically more favorable than the other two configurations EXO-8 and INT-16 (with interstitial F doping). Thus, only EXO-8 and EXO-16 configurations are discussed in detail in the following.

In all these configurations, the F atoms tend to stay on top sites of boron (B) atoms rather than on other possible sites

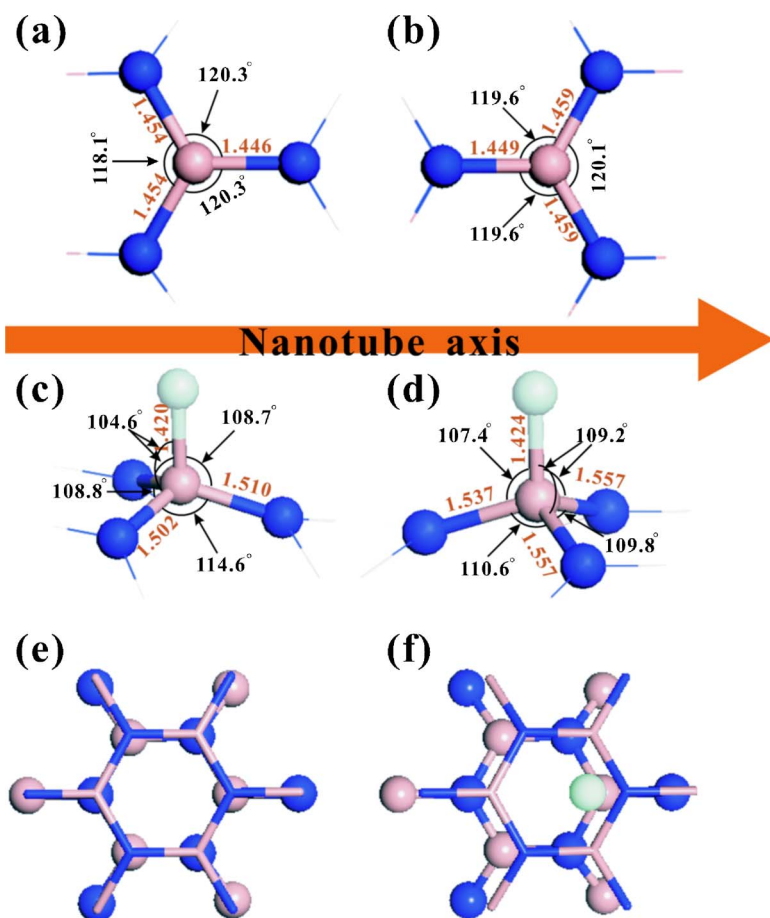


FIG. 2. (Color online) Bond lengths (in units of Å) and angles around the B site at the (a) inner and (b) outer walls of the pristine (8,0)–(16,0) DWBNNT. Bond lengths (in units Å) and angles around the adsorption site at (c) the inner wall of the EXO-8 configuration and (d) the outer wall of the EXO-16 configuration. The schematic diagrams of atomic arrangements of the pristine (8,0)–(16,0) DWBNNT and the EXO-8 configuration are shown in (e) and (f), respectively. The B, N, and F atoms are represented with the pink (dark gray), blue (black), and cyan (light gray) balls and sticks.

[such as top sites of nitrogen (N) atoms, bridge sites of BN bonds, and hollow sites of the hexagon]. The resulting distances between the F and B atoms are 1.420 and 1.424 Å for the EXO-8 and EXO-16 configurations, respectively. Compared with the pristine DWBNNTs, several considerable structural variations are observed in F-doped DWBNNTs. The first is that the F-doping configurations (EXO-8 and EXO-16) prefer pyramidalization (corresponding to sp^3 hybridization) to planar geometry (corresponding to sp^2 hybridization) around the adsorption site [as shown in Figs. 2(a)–2(d)]. In detail, all the B atoms bonded with the F atoms are displaced, and the related B–N bond lengths are elongated by about 0.05–0.10 Å. Correspondingly, most of the bond angles approach $109^\circ 28'$ (the ideal value of sp^3 hybridization). Note that this local transformation from sp^2 to sp^3 hybridization has been reported for fluorinated h -BN(001) plane²⁶ and SWBNNT.¹⁰ The other two structural features are only presented in the EXO-8 configuration. One feature is that the interstitial F doping leads to a modification of the “partial A-B stacking order” [each B or N atom in the inner tube faces a N or B atom in the outer tube, as shown in Fig. 2(e)] of the pristine DWBNNT.¹³ For the EXO-8 configuration, the F atom is bound to a B atom in the inner tube and then faces the middle point between two B atoms in the outer tube, as shown in Fig. 2(f). The other feature is that the B and N atoms in the outer shell (near the F atoms) radially move outwards, and thus, the outer shell buckling increases to about 0.15 Å. The minimum distance between the F atom and neighboring B atoms in the outer

wall is only 2.16 Å, smaller than the average spacing (3.24 Å) between two tube walls of the pristine DWBNNT.

To obtain physical and chemical insight into interstitial F doping in the EXO-8 configuration, the electron localization function²⁷ is calculated. The results show that the F atoms in the interstitial region directly interact with the B atoms in the inner tube with polarized covalent bonds [as shown by the arrow in Fig. 3(a)], whereas no covalent bond is formed between the F atoms and the outer (16,0) tube [as shown by the arrow in Fig. 3(b)]. Instead, there exists a weak electrostatic interaction between the F atom and the constituent atoms of the outer wall, since the minimum distance between them is only 2.16 Å and the Bader analysis²⁸ of the charge density

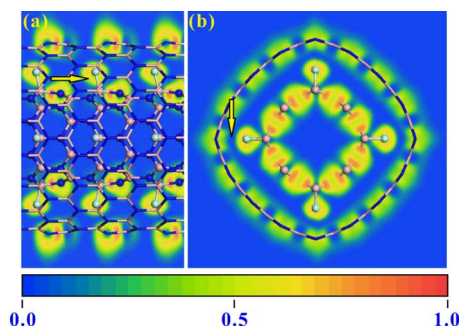


FIG. 3. (Color online) Contour plots of electron localization function of the EXO-8 configuration [interstitially F-doped (8,0)–(16,0) DWBNNT]. The side and perspective views are shown in (a) and (b), respectively.

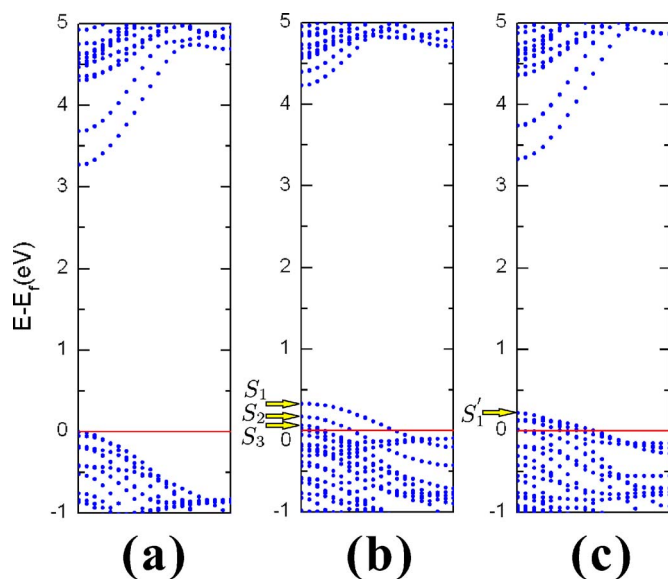


FIG. 4. (Color online) Band structures of (a) the pristine (8,0)–(16,0) DWBNNT, (b) the interstitially F-doped (8,0)–(16,0) DWBNNT (the EXO-8 configuration), and (c) the (8,0)–(16,0) DWBNNT with F adsorbed on the exterior surface of the (16,0) tube (the EXO-16 configuration). The Fermi energy (E_F) is set to zero. S_1 , S_2 , and S_3 denote the first, second, and third highest partially occupied bands across the Fermi level of the EXO-8 configuration, respectively. The S'_1 is the highest partially occupied band across the Fermi level of the EXO-16 configuration.

yields a charge transfer of $0.27e$ per F atom from the outer tube. Evidently, in comparison with the well-defined multipolar interaction in the pristine DWBNNT, the mechanism of interwall interaction in the EXO-8 configuration is significantly changed and is more complicated. Considerable charge transfer from the inner tube to the F atoms,²⁹ corresponding to more charge accumulation in the region between the two tube walls, could enhance the multipolar interwall interaction in F-doped DWBNNTs. Such an enhancement is consistent with the significant structural changes in the EXO-8 configuration as mentioned above.

The enhanced interwall interaction will result in some meaningful changes in the electronic properties of F-doped DWBNNT. Figure 4 shows the fundamental band structures of both pristine and F-doped (8,0)–(16,0) DWBNNTs. In pristine DWBNNTs, consistent with its negligible influences on the geometrical structure, the multipolar interwall interaction does not change the essential characteristics of electronic properties of each wall [shown in Fig. 4(a)]: there still exists a wide band gap, although it is slightly smaller than that of the inner (8,0) tube. Furthermore, the top of the valence bands and the bottom of the conduction bands are originated from the outer (16,0) and inner (8,0) nanotubes, respectively. These results are in good agreement with the previous theoretical study.¹³ In the band structures of F-doped DWBNNTs [shown in Figs. 4(b) and 4(c)], several bands are across the Fermi level and thus are partially occupied, indicating an enhancement of electrical conductivity.

It should be noted that the conduction mechanisms of these two configurations of F-doped DWBNNTs are dis-

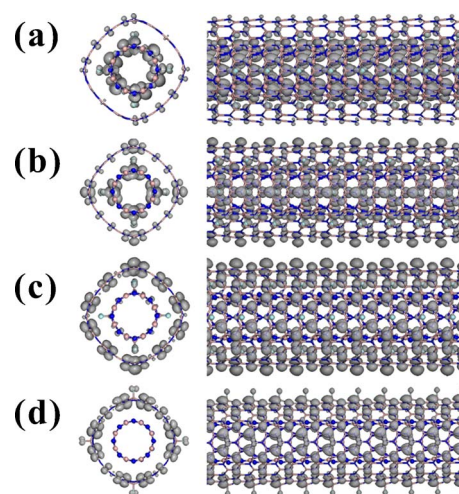


FIG. 5. (Color online) Isosurface plots of the squared wave function at the Γ point of partially occupied bands: (a) S_1 , (b) S_2 , (c) S_3 , and (d) S'_1 . In each panel, the perspective and side views are shown in the left and right, respectively. The isovalue is $0.005 e/\text{\AA}^3$. Note that the S_1 , S_2 , S_3 , and S'_1 have been defined in the Fig. 4. The B, N, and F atoms are represented with the pink, blue, and cyan balls and sticks.

tinctly different in essence, due to different origins and characteristics of these partially occupied bands. In the EXO-8 configuration, the electronic state of the topmost partially occupied band across the Fermi level, S_1 , is mainly distributed around the N sites of the inner (8,0) tube [as shown in Fig. 5(a)]. The electronic states of some other partially occupied bands (e.g., band S_3) are mainly distributed around the N sites of the outer (16,0) tube, as shown in Fig. 5(c). More interestingly, one partially occupied band, S_2 , is mainly composed of the π states around the N atoms in *both* inner (8,0) and outer (16,0) tubes [as shown in Fig. 5(b)], which corresponds to an enhanced interwall interaction. The above results indicate a transition from insulating to conducting behavior for both inner and outer tube walls of DWBNNT under interstitial F doping, where the interstitial F atoms play a role as a “bridge” between neighboring tube walls. Therefore, a significant enhancement of electrical conductivity for F-doped MWBNNTs can be derived in this manner.

In contrast, in the EXO-16 configuration, all partially occupied bands [e.g., S'_1 , as shown in Fig. 5(d)] are mainly contributed by the π states around the N atoms in the outer (16,0) tube, accompanied with a minor contribution from the p states around the F atoms. It implies that the F adsorption only changes the electrical properties of the outer tube from insulating to conducting and those of the inner tube are hardly affected and still insulating. It is compatible with the fact that F adsorption changes the outer tube’s curvature [shown in Fig. 1(d)], but the inner tube is less affected. This also suggests that the interwall interaction in this configuration is similar to that in the pristine DWBNNT. Then, the downshift of the Fermi level, induced by the electron transfer from the outer tube to the F atoms, gives rise to the presence of several partially occupied bands mainly contributed by the outer tube.

It should be noted that the above calculations are performed for the supercell configurations with a specific ar-

rament of F atoms. While it is important to check the effects induced by the choice of the supercell (size and doping configurations), test calculations are performed for (i) a similar supercell to the EXO-8 configuration but containing only two F atoms and (ii) a larger supercell containing two unit cells of the (8,0)–(16,0) BNNT and four F atoms, corresponding to a decrease of F-doping concentration by half. It is found that the test calculations yield similar characteristics of electronic structure to those of the EXO-8 configuration, revealing the same mechanism of fluorination-induced conductivity enhancement.

The above results suggest that the electronic properties of MWBNNTs can be modulated by adjusting the interwall interaction (for instance, interstitial doping with multivalent element and polar groups, or exerting high pressure).

IV. CONCLUSIONS

We have performed an *ab initio* investigation on the structural and electronic properties of the F-functionalized DWBNNT. The fluorination of DWBNNTs, where the F atoms are doped in the interstitial region between two neighboring tubes or adsorbed on the exterior surface of outer tube, is demonstrated as an exothermic process. In the case of interstitial F doping, the interwall interaction is significantly enhanced, distinctly different from that in pristine DWBNNTs. Correspondingly, the following apparent structural changes are observed: (i) the local transformation from sp^2 to sp^3 hybridization around the adsorption sites, and (ii) the enhancements of the bucklings of the tube walls and the

modification of the interwall stacking order. Interstitial F doping affects the electronic structure of doped DWBNNTs as a whole. In detail, interstitial F doping induces not only partially occupied bands distributed over either outer or inner tubes but also a new partially occupied band that is spatially distributed over both outer and inner tubes, which indicates that both walls of DWBNNTs become conducting together. In contrast, for the case of F adsorption on the exterior surface of outer tube of DWBNNT, only negligible influence on the interwall interaction can be induced by the adsorbed F atoms. The local deformation only occurs around the adsorption sites at the outer tube. Furthermore, the structure of the whole doped system can be deemed as that of a simple combination of a pristine inner tube and an outer tube adsorbed with F atoms. Correspondingly, all partially occupied bands are mainly originated from the outer tube, while the inner tube has no contribution to the electrical conductivity. In a word, interstitial F doping can provide more effective conducting channels than the F adsorption on the outmost shell of MWBNNTs and, therefore, a more significant enhancement of electrical conductivity for F-doped MWBNNTs can be achieved in this manner.

ACKNOWLEDGMENTS

This work was supported by the Ministry of Science and Technology of China (Grant No. 2006CB605105), the National Natural Science Foundation of China (Grants No. 10325415 and No. 10404016), and the Ministry of Education of China (Grant No. SRFDP 20050003085). We are thankful for computational support from THPCC.

*Author to whom correspondence should be addressed. Electronic address: dwh@phys.tsinghua.edu.cn

- ¹A. Rubio, J. L. Corkill, and M. L. Cohen, *Phys. Rev. B* **49**, 5081 (1994); X. Blase, A. Rubio, S. G. Louie, and M. L. Cohen, *Europhys. Lett.* **28**, 335 (1994).
- ²N. G. Chopra, R. J. Luyken, K. Cherrey, V. H. Crespi, M. L. Cohen, S. G. Louie, and A. Zettl, *Science* **269**, 966 (1995).
- ³R. Arenal, O. Stéphan, M. Kociak, D. Taverna, A. Loiseau, and C. Colliex, *Phys. Rev. Lett.* **95**, 127601 (2005).
- ⁴Y. Chen, J. Zhou, S. J. Campbell, and G. L. Caer, *Appl. Phys. Lett.* **84**, 2430 (2004).
- ⁵L. Wirtz, A. Marini, and A. Rubio, *Phys. Rev. Lett.* **96**, 126104 (2006); C.-H. Park, C. D. Spataru, and S. G. Louie, *ibid.* **96**, 126105 (2006).
- ⁶Y. H. Kim, K. J. Chang, and S. G. Louie, *Phys. Rev. B* **63**, 205408 (2001).
- ⁷K. H. Khoo, M. S. C. Mazzoni, and S. G. Louie, *Phys. Rev. B* **69**, 201401(R) (2004).
- ⁸X. Blase, J. C. Charlier, A. De Vita, and R. Car, *Appl. Phys. A: Mater. Sci. Process.* **68**, 293 (1999); W. Q. Han and A. Zettl, *J. Am. Chem. Soc.* **125**, 2062 (2003).
- ⁹C. C. Tang, Y. Bando, Y. Huang, S. L. Yue, C. Z. Gu, F. F. Xu, and D. Golberg, *J. Am. Chem. Soc.* **127**, 6552 (2005).
- ¹⁰H. J. Xiang, J. L. Yang, J. G. Hou, and Q. S. Zhu, *Appl. Phys. Lett.* **87**, 243113 (2005).

- ¹¹A. Loiseau, F. Willaime, N. Demoncey, G. Hug, and H. Pascard, *Phys. Rev. Lett.* **76**, 4737 (1996); D. Golberg, Y. Bando, M. Eremets, K. Takemura, K. Kurashima, and H. Yusa, *Appl. Phys. Lett.* **69**, 2045 (1996).
- ¹²D. Golberg and Y. Bando, *Appl. Phys. Lett.* **79**, 415 (2001).
- ¹³S. Okada, S. Saito, and A. Oshiyama, *Phys. Rev. B* **65**, 165410 (2002).
- ¹⁴S. H. Jhi, D. J. Roundy, S. G. Louie, and M. L. Cohen, *Solid State Commun.* **134**, 397 (2005).
- ¹⁵G. Y. Guo and J. C. Lin, *Phys. Rev. B* **72**, 075416 (2005).
- ¹⁶A. Bachtold, C. Strunk, J. P. Salvetat, J. M. Bonard, L. Forró, T. Nussbaumer, and C. Schönenberger, *Nature (London)* **397**, 673 (1999); P. G. Collins, M. Hersam, M. Arnold, R. Martel, and Ph. Avouris, *Phys. Rev. Lett.* **86**, 3128 (2001).
- ¹⁷S. Sanvito, Y.-K. Kwon, D. Tománek, and C. J. Lambert, *Phys. Rev. Lett.* **84**, 1974 (2000); Q. Yan, J. Wu, G. Zhou, W. Duan, and B.-L. Gu, *Phys. Rev. B* **72**, 155425 (2005).
- ¹⁸J. P. Perdew, K. Burke, and M. Ernzerhof, *Phys. Rev. Lett.* **77**, 3865 (1996).
- ¹⁹G. Kresse and J. Fürthmüller, *Comput. Mater. Sci.* **6**, 15 (1996); *Phys. Rev. B* **54**, 11169 (1996).
- ²⁰P. E. Blöchl, *Phys. Rev. B* **50**, 17953 (1994); G. Kresse and D. Joubert, *ibid.* **59**, 1758 (1999).
- ²¹D. Golberg, W. Han, Y. Bando, L. Bourgeois, K. Kurashima, and T. Sato, *J. Appl. Phys.* **86**, 2364 (1999); D. Golberg, Y. Bando,

- K. Kurashima, and T. Sato, *Chem. Phys. Lett.* **323**, 185 (2000).
- ²²H. J. Monkhorst and J. D. Pack, *Phys. Rev. B* **13**, 5188 (1976).
- ²³The geometrical structure of the pristine (8,0)–(16,0) DWBNNT is shown in Figs. 1(a), 2(a), and 2(b). The average radii for the inner and outer tubes are 3.22 and 6.46 Å, respectively. Consequently, the average spacing between two tube walls is 3.24 Å, which is slightly smaller than the experimental value of 3.3 ~ 3.4 Å (Ref. 11). Moreover, the bucklings for the inner and outer tube are 0.07 and 0.04 Å, respectively.
- ²⁴In this paper, only the F adsorption is taken into account owing to the following reasons: It has been pointed out by Xiang *et al.* (Ref. 10) that F-substitutional doping in SWBNNT does not provide a reasonable explanation for the significant enhancement of electric conductance observed in the experiment. We have also examined the F-substitutional doping with our DWBNNT model, where several different F contents are considered. The obtained results show that the sufficient enhancement of electric conductance is unlikely to be achieved until the doped tube wall is destroyed permanently by too many substitutional F atoms.
- ²⁵The binding energy is defined as $\Delta E = [E(\text{BNNT} + n\text{F}) - E(\text{BNNT}) - nE(\text{F})]/n$, where $E(\text{BNNT} + n\text{F})$, $E(\text{BNNT})$, and $E(\text{F})$ are the total energies of the (8,0)–(16,0) DWBNNT doped with n F atoms per unit cell, the isolated (8,0)–(16,0) DWBNNT, and the F atom, respectively, and n is the number of F atoms doped in the DWBNNT.
- ²⁶B. Mårlid, K. Larsson, and J.-O. Carlsson, *J. Phys. Chem. B* **103**, 7637 (1999).
- ²⁷The electron localization function (ELF) provides a good description of polycentric bonding in a structural complex as a function of the real-space coordinates. The value of the ELF ranges between 0 and 1. Generally, higher value of ELF implies a lower Pauli kinetic energy, which occurs in localized covalent bonds or lone electron pairs, and ELF=1 corresponds to perfect localization. For details of ELF, see A. D. Becke and K. E. Edgecombe, *J. Chem. Phys.* **92**, 5397 (1990); S. Noury, F. Colonna, A. Savin, and B. Silvi, *J. Mol. Struct.* **450**, 59 (1998).
- ²⁸G. Henkelman, A. Arnaldsson, and H. Jónsson, *Comput. Mater. Sci.* **36**, 354 (2006).
- ²⁹J. Li, G. Zhou, H. T. Liu, and W. H. Duan, *Chem. Phys. Lett.* **426**, 148 (2006).